correction. Reasonable estimations of systematic effects seem to be adequate for the successful application of this method of locating light atoms. In its original application to n-propylarsonic acid, (Smith, Zingaro & Meyers, 1971) a computer program was modified to allow the calculation of weighted difference syntheses, but a mistake was made in the programming. This may be responsible for the lack of success of the method in that case.

We wish to thank the Robert A. Welch Foundation, Houston, Texas, for financial support during the development of the method.

References

ARGOS, P. & CLAYTON, R. (1973). *Acta Cryst.* B**29**, 910–913.
DENTON, D. L., CLAYTON, W. R. & SHORE, S. G. (1974). Submitted for publication.
SMITH, M. R., ZINGARO, R. A. & MEYERS, E. A. (1971). *J. Organometal. Chem.* **27**, 341–347.
WOODWARD, P. M. (1953). *Probability and Information Theory with Applications to Radar*. New York: McGraw-Hill.
X-RAY System (1972). Technical Report TR-192 of the Computer Science Center, Univ. of Maryland. Version of June 1972.

Acta Cryst. (1975). A**31**, 746

Calculated Images of Crystal Lattices by Axial Illumination with 1 MeV Electrons

BY A. BOURRET, J. DESSEAUX AND A. RENAULT

Centre d'Etudes Nucléaires de Grenoble, Département de Recherche Fondamentale, Section de Physique du Solide, BP 85 *Centre de Tri*, 38041 *Grenoble Cedex, France*

(*Received* 11 *February* 1975; *accepted* 28 *March* 1975)

Multibeam (001) electron-microscope lattice-image ($N=3,5$) properties are studied when axial illumination is used. Numerical calculations were particularly applied to (001)-oriented gold foils observed with 1 MeV electrons. Conditions for obtaining images showing no artificial periodicity are determined. It is shown that in a particular range of thickness (40–60 Å for three-beam interference or 70–120 Å for five-beam interference) and with the proper defocusing distance high-contrast images would be obtained: the exact projected atomic positions are directly visible on these images. The influence of departure from exact symmetry conditions, and of large variation of the lattice parameter, are also studied. These calculations suggest that it would be possible to observe direct lattice images of metals and to study their defects with actual 1 MeV electron microscopes.

1. Introduction

Lattice fringe images are commonly produced by interference of two beams either with axial illumination or with a tilted illumination. As demonstrated by several authors (Dowell, 1963; Cockayne, Parsons & Hoelke, 1971), these procedures give a displacement of the fringes relative to the atomic position, which is a function of several parameters (spatial frequency, specimen thickness of Bragg deviation). Therefore this procedure is not suitable to obtain an image which reproduces the projected potential, and direct correlation between the object and the image intensity is not valid.

On the other hand for weak phase objects, observed with axial illumination and symmetrical diffraction conditions the transfer between phase changes in the object and intensity in the image is linear and there is no lateral shift apart from contrast inversion (Hanszen, 1971). In contrast, in a strong phase object (such as a crystal) the transfer is no longer linear. Nevertheless, the lateral shift is still zero when symmetrical diffraction conditions are concerned (Laue position) and the image can be interpreted in terms of the crystal structure as shown by Cowley & Iijima (1972). These properties were applied extensively to study large unit cells of complex oxide structure with 100 keV electrons (Allpress & Sanders, 1973). But because of the spherical aberration of the objective lens, the maximum scattering angle is limited. The desirable cut-off angle and optimum defocus appear to be given by Scherzer's (1949) conditions. With the available 100 keV electron microscope the optimum resolution determined by these conditions is limited to approximately 3 Å: in complex oxides where distances between metal atom columns larger than 3·8 Å are clearly resolved this limit is nearly attained.

The use of 1 MeV electrons seems to be a powerful means to increase the resolution: the optimum resolution given by Scherzer's conditions is of the order of 1·2 Å with actual objective lenses so that imaging of atomic columns closer than 3 Å is possible. In partic-

ular, in pure metals, where interplanar distances are smaller than 3 Å, axial illumination is only possible with 1 MeV electrons.

The resolution at atomic level of a perfect lattice in a metal has no interest *per se*, as there is no problem of crystalline structure. Nevertheless it would be very interesting to study the imperfect crystal at this level. Among different imperfections the one which offers the most direct interpretation is an end-on defect occupying all the thickness of the foil: in this case the atomic columns lie in the same direction as in the perfect crystal and are everywhere parallel to the beam. Edge dislocations viewed end-on and planar defects viewed end-on, such as grain boundaries or phase boundaries, offer examples of this type of defect.

The purpose of this study is to determine theoretically:

(i) What are the best experimental conditions to obtain a one-to-one correspondence between the image and the object even with non-linear transfer.

(ii) The imaging conditions which give a correct image with high contrast.

(iii) The sensitivity of these images to chromatic aberration or departure from the exact symmetrical diffracting condition.

(iv) The effect of changing the lattice parameter to simulate what happens near an end-on defect occupying all the thickness of the foil.

The case of (001) oriented single crystals of gold has been chosen for numerical application, as these films are well suited for experimental observations and easily prepared at small and controlled thickness.

2. Method of calculation

Below the object the total wave amplitude at a point defined by **r** is given by:

$$\Psi=\sum_g U_g \exp i\varphi_g \exp 2\pi i\mathbf{g}\,.\,\mathbf{r}+U_o \exp i\,\varphi_o$$

where U_o, U_g are the amplitudes of the transmitted and scattered waves and φ_o, φ_g their respective phases.

The phase change between the O beam and the G beam due to spherical aberration and defocus, which occurs in the objective lens, is given by (Hanszen, 1971):

$$\Phi_g-\Phi_o=\frac{2\pi}{\lambda}\left[C_S\frac{\alpha_g^4}{4}+\frac{\Delta z\,\alpha_g^2}{2}\right] \qquad (1)$$

where $\alpha_g=g\lambda$ is the angle between the O beam and the G beam supposing that the O beam is along the optical axis. C_S is the spherical aberration coefficient. Δz is the defocusing distance.

Therefore the total wave amplitude in the image plane (for unit magnification) is:

$$\psi=U_o \exp i(\varphi_o+\phi_o)+\sum_g U_g \exp 2\pi i\mathbf{g}\,.\,\mathbf{r} \exp i(\varphi_g+\phi_g),$$

where the sum over g is extended over all the beams included in the objective aperture.

In the Laue position $U_g=U_{-g}$, $\varphi_g=\varphi_{-g}$ and ψ reduces to:

$$\psi=U_o \exp i(\varphi_o+\phi_o)+2\sum_{g>0}^{|g_{max}|} U_g \cos 2\pi\mathbf{g}\,.\,\mathbf{r} \exp i(\varphi_g+\phi_g)$$

and the intensity in the image plane is:

$$\begin{aligned} I_N=\psi\psi^*=U_o^2&+4\sum_{g>o}^{|g_{max}|} U_g^2\cos^2 2\pi\mathbf{g}\,.\,\mathbf{r}\\ &+4\sum_{g>o}^{|g_{max}|} U_gU_o\cos 2\pi\mathbf{g}\,.\,\mathbf{r}\cos[\phi_g-\phi_o+\varphi_g-\varphi_o]\\ &+8\sum_{|\mathbf{g}|=|\mathbf{g}'|}^{|g_{max}|} U_g^2\cos 2\pi\mathbf{g}\,.\,\mathbf{r}\cos 2\pi\mathbf{g}'\,.\,\mathbf{r}\\ &+8\sum_{|\mathbf{g}|>|\mathbf{g}'|}^{|g_{max}|} U_gU_{g'}\cos 2\pi\mathbf{g}\,.\,\mathbf{r}\cos 2\pi\mathbf{g}'\,.\,\mathbf{r}\\ &\times\cos[\phi_g-\phi_{g'}+\varphi_g-\varphi_{g'}]\,. \end{aligned} \qquad (2)$$

Numerical calculations have been performed applying (2) for two typical cases: three-beam interference on a systematic [200] row in order to image atomic planes, and five-beam interference on a systematic (001) plane to image atomic columns. The phase and amplitude of the beams included to form the image are calculated by N-beam dynamical theory in the matrix formulation without absorption (Howie & Whelan, 1961). In both cases the important question arises of how many beams must be included in the calculation. This has been studied in the following two ways:

(i) eigenvalues of the three main Bloch waves are calculated for different numbers of beams until a steady value is reached.

(ii) amplitudes of the five main diffracted beams at the bottom of the foil are evaluated as a function of foil thickness for an increasing number of beams. This number of beams is assumed to be sufficient when the variation of the amplitudes of the five main beams becomes negligible (foil thickness limited to 200 Å). These criteria lead to the same great number of beams especially in the case of a systematic (001) plane: but the high symmetry of the Laue position permits the reduction of the rank of the matrix to be diagonalized.

3. Imaging of atomic planes: three-beam interference

Three-beam interference has been treated in detail by Komoda (1964). Particularly for axial illumination Komoda shows that general properties of the image are:

(i) The interference fringes are composed of two components: one has the periodicity of lattice planes and the other half this periodicity.

(ii) The half-periodicity component is achromatic, but the other is sensitive to defocus.

(iii) In the symmetry position, the location of atomic plane is either at a maximum or half way between two maxima of the intensity profile, depending of the defocusing distance.

Nevertheless Komoda's analysis is incomplete in respect of quantitative interpretation because spherical aberration was neglected and the amplitude of the beams was calculated in the two-beam approximation. In that sense, at 1 MeV, quantitative evaluation must be performed for each particular material and orientation.

In the case of three-beam interference with $\pm G$ on a systematic row, the image intensity given by (2) reduces to:

$$I_3 = U_o^2 + 4U_g^2 \cos^2 2\pi gr + 4U_g U_o T(g,\Delta z) \cos 2\pi gr \quad (3)$$

where

$$T(g,\Delta z) = \cos(\phi_g - \phi_o + \varphi_g - \varphi_o)$$

and the function $T(g,\Delta z)$ gives the variation of contrast due to all the phase changes (aberrations and dynamical diffraction). In gold dynamical calculations were performed with 17 beams although good values of amplitudes and phases had already been obtained with seven beams (error not exceeding 5%) [Fig. 1(*a*) and (*b*)]. At small thickness one effective extinction distance of 180 Å due to interference between Bloch wave 2 and Bloch wave 3 dominates.*

3.1 *Optimum thickness*

As is clear from (3), the profiles have maximum or minimum intensity at $r=0$ (atomic plane position) depending on the sign of $T(g,\Delta z)$ for thicknesses where $U_o \gg 2U_g$. On the other hand, when $U_o \ll 2U_g$ the profiles have half-periodicity and are rather insensitive to variation of $T(g,\Delta z)$.

If the contrast, C, is defined as usual as

$$C = 2\frac{I_{max} - I_{min}}{I_{max} + I_{min}},$$

maximum contrast of the fringes ($C=2$) occurs when $U_o < 2U_g$. But when $U_o < U_g$ an undesirable half-periodicity is predominant and the optimum thickness is found for $U_g < U_o < 2U_g$, *i.e.* in the region 40–60 Å or 120–140 Å.

A series of typical intensity profiles is shown in Fig. 2. The maximum intensity is $2{\cdot}5\,I_o$ instead of the value $3I_o$ which would have been obtained if the beams stopped by the aperture had been neglected.

3.2 *Variation with defocusing*

The effect of defocusing is governed by the term $T(g,\Delta z)$ of equation (3). This term must be equal to

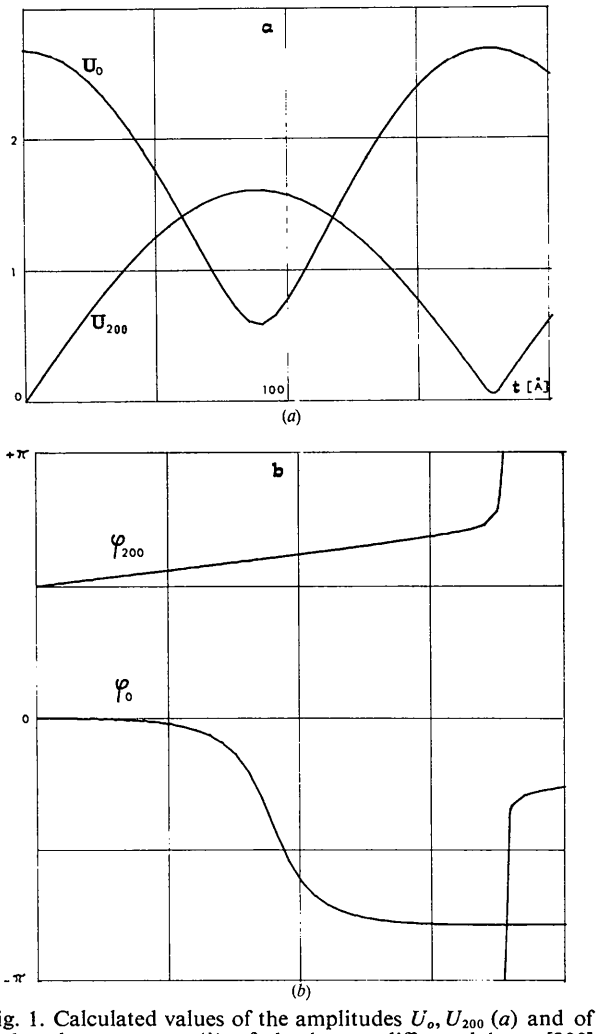

Fig. 1. Calculated values of the amplitudes U_o, U_{200} (*a*) and of the phases φ_o, φ_{200} (*b*) of the beams diffracted by a [200] systematic row in gold as a function of crystal thickness ($E=1$ MeV, 17-beam calculation.)

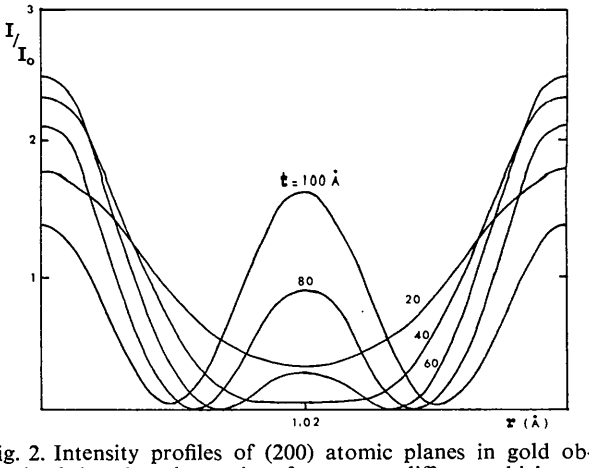

Fig. 2. Intensity profiles of (200) atomic planes in gold obtained by three-beam interference at different thickness. Constant defocus set at −700 Å. ($E=1$ MeV).

* Bloch waves are numbered from their corresponding eigenvalue. (The greatest eigenvalue is numbered 1 and so on.)

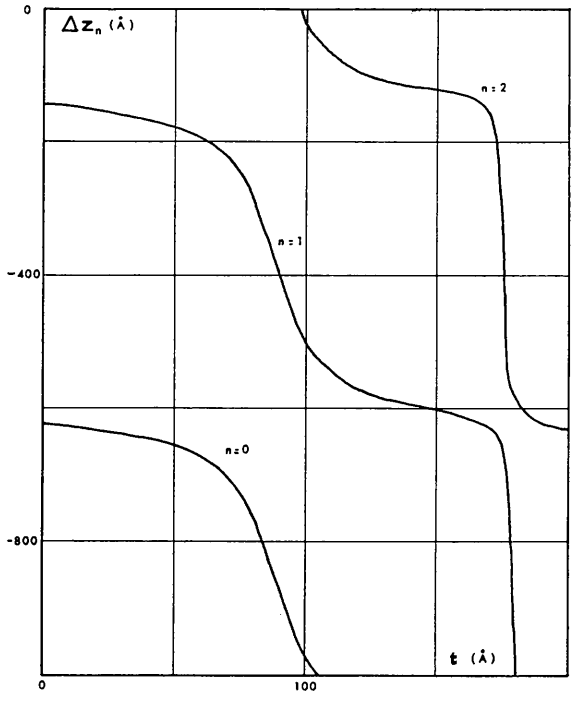

Fig. 3. Defocusing distance Δz_n at which optimum contrast occurs as a function of thickness in gold. Three-beam interference on a [200] systematic row. For n even, intensity maxima are located at atomic plane position and for n odd at half distance between two atomic planes.

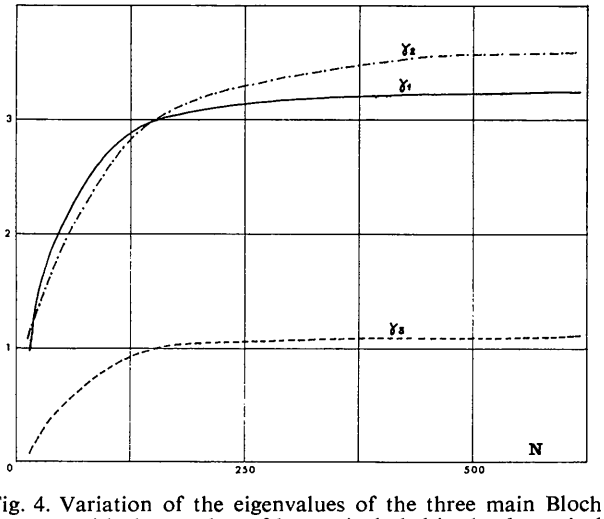

Fig. 4. Variation of the eigenvalues of the three main Bloch waves with the number of beams included in the dynamical interaction on a (001) systematic plane in gold. γ_1 is multiplied by a factor of 10^{-2} and γ_2 and γ_3 by a factor of 10^{-3}. The vertical scale is in $Å^{-1}$.

± 1 to give maximum amplitude to the cos $2\pi gr$ term. For very small thickness, where $\varphi_g-\varphi_o=\pi/2$ it reduces to $T(g,\Delta z)=-\sin(\phi_g-\phi_o)$, which is the well known transfer function for weak phase objects. But it is important to note that, even when the object can no longer be considered as a weak phase object, there is an appropriate defocusing distance for which contrast is a maximum. This condition is obtained when:

$$\phi_g-\phi_o+\varphi_g-\varphi_o=n\pi\,,$$

when n is an integer, giving the appropriate defocus Δz_n:

$$\Delta z_n=\frac{2}{g^2\lambda}\left[\frac{n}{2}-\frac{\varphi_g-\varphi_o}{2\pi}\right]-C_S\frac{g^2\lambda^2}{2}\,. \tag{4}$$

If $n=2k$, the contrast is positive, *i.e.* intensity maxima are located at the atomic plane projections.

If $n=2k+1$, the contrast is negative, *i.e.* intensity maxima are located half way between the atomic plane projections.

Fig. 3 shows the different Δz_n values in the [200] systematic row in gold at different thicknesses, from which interpretation of an image is easy when defocusing distance and foil thickness are known.

The successive Δz_n values are not equivalent: for partially coherent illumination Frank (1973) has shown that the transfer is not affected by illumination aperture when

$$\Delta z_a\simeq -C_S g^2\lambda^2 \tag{5}$$

(it can be demonstrated easily that this result still holds in the case of three-beam interference). The n value must thus be chosen so that Δz_n is as close as possible to $\Delta z_a=-764$ Å.

The voltage and current fluctuations which produce instabilities of Δz reduce the mean value of $T(g,\Delta z)$ and affect the periodicity $1/g$. When, for example, the results of Hanzen & Trepte (1971) are applied instabilities have negligible effect if

$$\pi g^2\lambda\Delta\tilde{z}<1\,,$$

where $\Delta\tilde{z}$ is the amplitude of a sinusoidal fluctuation. This gives $\Delta\tilde{z}<150$ Å, which is obtainable on a well stabilized electron microscope.

3.3. *Influence of asymmetry of the diffraction condition*

Departure from exact symmetry conditions will modify the intensity profiles. In this case $U_g\neq U_{-g}$ and $\varphi_g\neq\varphi_{-g}$ and the profiles are displaced relative to the atomic position. Computer calculations have been performed at different incident directions from the Laue position to the Bragg position on the 400 diffracted beam (rotation of $2\theta_B$).

The main result, summarized in Table 1, is that the relative displacement does not depend linearly on the deviation angle from the Laue position, nor on the thickness of the specimen. Up to a thickness of 100 Å, rotation of $\pm 2\theta_B$ is permissible.

Table 1. *Displacement of the maximum of intensity profile in % of the lattice parameter as a function of thickness at different deviation angles (in units of θ_B) from the Laue position*

[200] systematic row in gold–1 MeV

Deviation from Laue position	50	100	150 (Å)
0·5 θ_B	1·5	4·5	12%
1·0	2·5	8	unobservable
1·5	4	10	unobservable
2·0	5	12	unobservable

4. Imaging of atomic columns

If the image is formed with the crystal oriented on a systematic (001) plane, images of projected atomic columns result from five-beam interference (200-type diffracted beams). Another possibility would have been nine-beam interference including 200 and 220-type diffracted beams. But this type of interference seems to be of negligible practical interest as the image is very sensitive to focusing or exact specimen thickness.

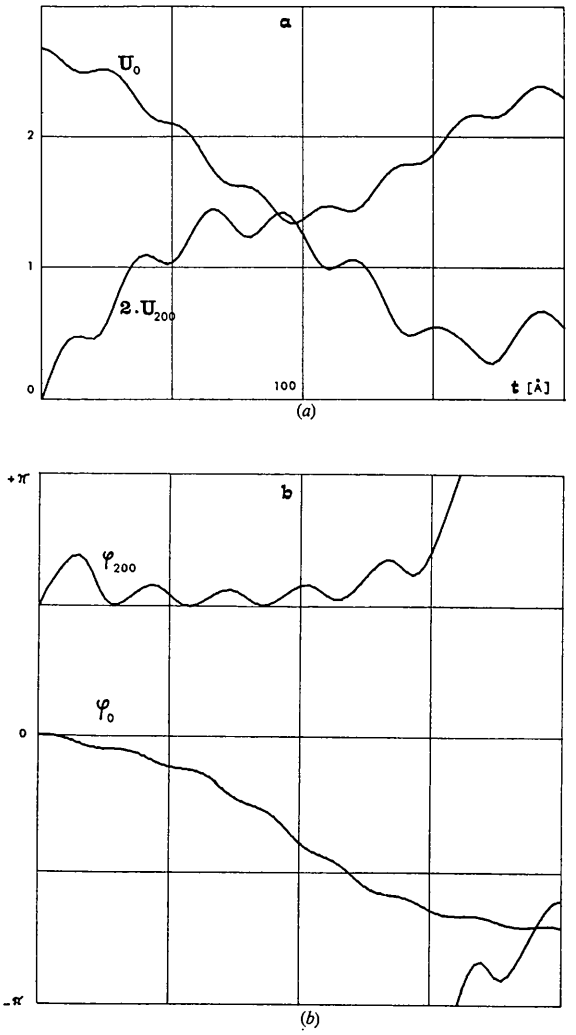

Fig. 5. Calculated values of the amplitudes $U_o, 2U_{200}$ (*a*) and of the phases φ_o, φ_{200} (*b*) of the beams diffracted by a (001) systematic plane in gold as a function of crystal thickness.

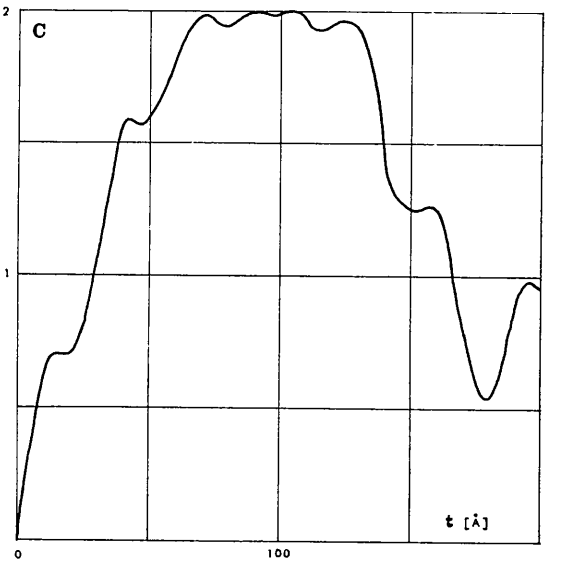

Fig. 6. Contrast C, of (001) atomic column images (five-beam interference) as a function of thickness in gold. ($E=1$ MeV). The contrast has been calculated at the optimum defocus Δz_n at every thickness.

In the five-beam case the formula (2) reduces to

$$I_5 = U_o^2 + 4U_g^2 (\cos 2\pi \mathbf{g}_{20}\mathbf{r} + \cos 2\pi \mathbf{g}_{02}\mathbf{r})^2 + 4U_g U_o T(g, \Delta z)(\cos 2\pi \mathbf{g}_{20}\mathbf{r} + \cos 2\pi \mathbf{g}_{02}\mathbf{r}) \quad (6)$$

which is very similar to (3) and therefore has the same properties: the contrast is maximum if $2U_g \simeq U_o$ and $T(g, \Delta z) = \pm 1$.

Amplitudes U_o, U_{200} and phases φ_o, φ_{200} were dynamically calculated with 613 diffracted beams (which reduce by symmetry to a 89×89 matrix) or 314 (which reduce to a 49×49 matrix). Results obtained with these two values are very similar, showing that the asymptotic value for large N has been attained (Fig. 4). Fig. 5 shows the influence of thickness: two main effective extinction distances are visible at small thickness at 200 Å (Bloch waves 1 and 3) and 31 Å (Bloch waves 1 and 2).

4.1. *Optimum thickness*

The region where $2U_g \simeq U_o$ is situated around 90 Å but the contrast is not very sensitive to the thickness as is illustrated in Fig. 6. In practice, from 70 to 130 Å contrast is very close to its maximum value, $C=2$. Therefore five-beam interference must be used in foils of intermediate thickness in a region where three-beam interference is dominated by the half-periodicity term.

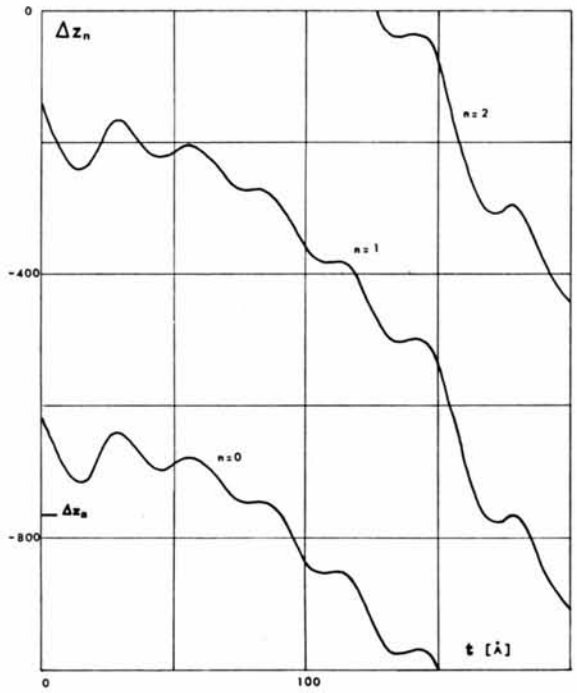

Fig. 7. Defocusing distance Δz_n at which optimum contrast occurs as a function of thickness. Five-beam interference on the (001) systematic plane in gold ($E=1$ MeV). For n even the intensity maxima are located at the projections of the atomic columns. For n odd the intensity maxima are situated at positions $\frac{1}{2},\frac{1}{2}$ of the cubic projected lattice.

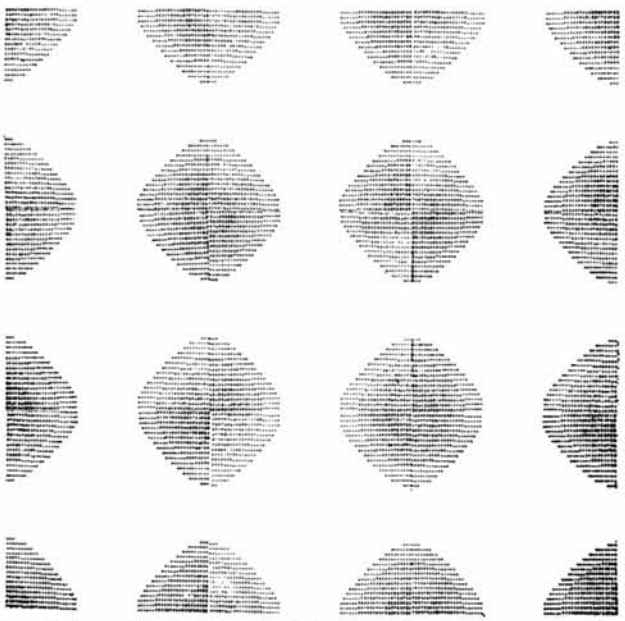

Fig. 8. Simulated images resulting from five-beam interference on the (001) systematic plane in gold. All four beams of 200 type are included. Darker parts represent higher intensity and are located at the projection of atomic columns forming a simple cubic lattice of parameter 2·04 Å, $t=60$ Å, $\Delta z=-700$ Å.

4.2. *Variation with defocusing distances*

The effect of defocus is very similar to the three-beam interference. Contrast is maximum for particular value Δz_n given by (4) (Fig. 7). When $n=2k$ the intensity maxima are located at atomic column projections forming a square pattern, and when $n=2k+1$ the intensity maxima are situated at position $\frac{1}{2},\frac{1}{2}$ of the cubic projected lattice (Fig. 8). It is worth while to note that for $n=0$ the optimum defocus for thicknesses up to 100 Å is very close to Δz_a given by (5), and hence the illumination divergence has negligible effect.

4.3. *Stability of the image for variation of g*

Near a defect such as an end-on edge dislocation or a perpendicular grain boundary the lattice parameter changes in the plane of the foil: this rather unusual situation, where the displacement of atoms **R** does not depend on the position in a column parallel to the beam, is the simplest one. It is the only way to obtain direct quantitative information about **R** from the image.

The proposed treatment is based on the column approximation: a new unit quadratic cell is locally considered with no variation along (001). Dynamical equations are solved with this new cell and using (6) the image of the local lattice is calculated. The validity of this approximation is supported by the fact that foil thickness is restricted to a low value. For instance for a 50 Å thick foil, using Takagi's (1962) triangle the maximum area at the top of the foil contributing to the amplitude of the wave at a point of the bottom surface would have a diameter of 4 Å (including beams up to the 10th order). This represents only two atomic distances over which the deformation has to be considered as constant.

In the five-beam case inspection of formula (6) shows that two conditions are required for a direct read out of the structure:

(i) variation of $T(g,\Delta z)$ has to remain small over large change of g;

(ii) dynamical conditions have to be relatively stable, especially phases $\varphi_g-\varphi_o$.

For a thick specimen, this second condition is difficult to realize. Dynamical calculation shows that up to a thickness of 100 Å the variation of $\varphi_g-\varphi_o$ is inferior to $0{\cdot}17\pi$ for $|\Delta g|/|g|=50\%$. Then the first condition reduces to a proper choice of the defocusing distance: the distance Δz_a given by (5) must be chosen as it ensures the best stability of $T(g,\Delta z)$ (first and second derivative relative to g are then equal to zero).

Simulated image profiles calculated for different values of the lattice parameter of a quadratic unit cell are given in Fig. 9 for a foil thickness of 50 Å. The contrast does not change when $d_{200}=d_{020}$ varies between 1·6 Å and 3·0 Å. The image reproduces very well the projected structure at large positive dilatation (expansion), but is rather sensitive for negative dilata-

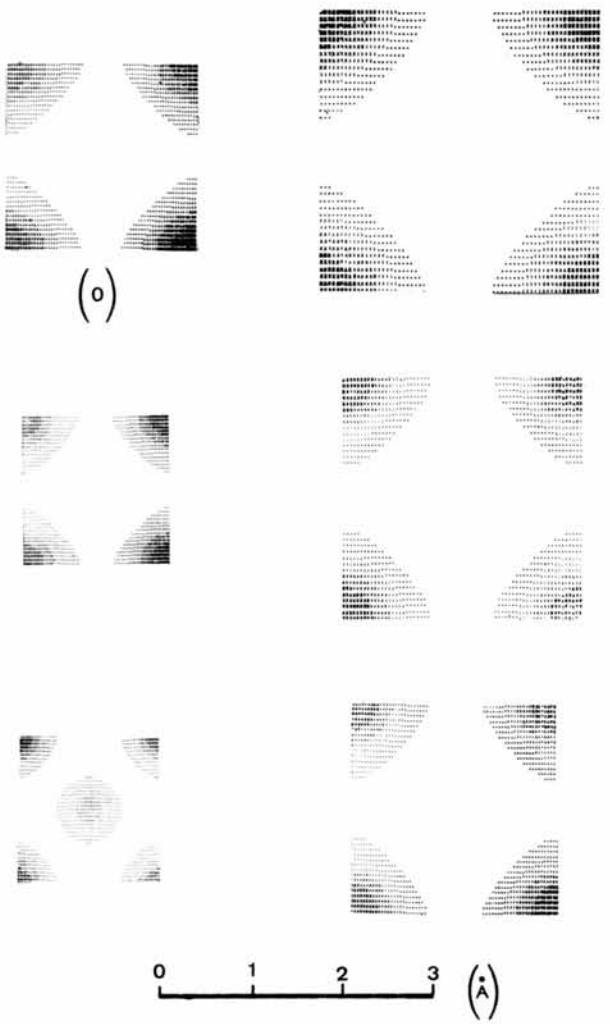

Fig. 9. Simulated images of atomic columns in a (001), five-beam interference. The gold structure is supposed to be dilated so that d_{002} remains constant but $d_{200} = d_{020}$ varies, the unit cell being quadratic. Each square size is proportional to the d_{200} value. The case (O) corresponds to the non-deformed gold structure. The image remains constant except for $d_{200} < 1{\cdot}6$ Å. Constant defocus set at -760 Å.

tion. This confirms the intuitive view that direct read out of the structure can only be obtained for distances between atomic columns larger than the resolution.

5. Conclusion

The observation of lattice fringes or multibeam interference images directly related to the object is possible with actual 1 MeV electron microscopes.

The exact interpretation of the images necessitates a good knowledge of the thickness of the object and of the defocusing distance. Numerical application on (001) gold foil shows that optimum thickness for observing (200) atomic planes is 40–60 Å or 120–140 Å, and for observing [001] atomic columns is 70–130 Å.

The exact Laue condition has to be more and more precisely defined with increasing thickness, but will be easily obtained in gold in the thickness range 50–100 Å.

Furthermore large variation of the lattice parameter (especially in expansion) can be detected directly in the image, suggesting that, for very small thicknesses (~ 60 Å max), direct read out of the projected structure of some defects will be obtained from electron micrographs.

References

ALLPRESS, J. G. & SANDERS, J. V. (1973). *J. Appl. Cryst.* **6**, 165–190.
COCKAYNE, D. J. H., PARSONS, J. R. & HOELKE, C. W. (1971). *Phil. Mag.* **24**, 139–153.
COWLEY, J. M. & IIJIMA, S. (1972). *Z. Naturforsch.* **27a**, 445–451.
DOWELL, W. C. T. (1963). *Optik*, **20**, 535–568.
FRANK, J. (1973). *Optik*, **38**, 519–536.
HANSZEN, K. L. (1971). *Advanc. Opt. Electron Microsc.* **4**, 1–82.
HANSZEN, K. L. & TREPTE, L. (1971). *Optik*, **32**, 519–538.
HOWIE, A. & WHELAN, M. J. (1961). *Proc. Roy. Soc.* A **263**, 217–237.
KOMODA, T. (1964). *Optik*, **21**, 93–110.
SCHERZER, O. (1949). *J. Appl. Phys.* **20**, 20–29.
TAKAGI, S. (1962). *Acta Cryst.* **15**, 1311–1312.